Design Rules for High-Performance FARAD Thrusters

IEPC-2005-207

Presented at the 29th International Electric Propulsion Conference, Princeton University
October 31 – November 4, 2005

Kurt A. Polzin* and Edgar Y. Choueiri†
Electric Propulsion and Plasma Dynamics Laboratory (EPPDyL)
Mechanical and Aerospace Engineering Department
Princeton University
Princeton, New Jersey 08544

A set of design rules aimed at producing a high-performance Faraday Accelerator with Rf-Assisted Discharge (FARAD) are derived using previous modeling results and insight into the underlying physical processes. The rules concern the optimization of each of the major processes in the FARAD: plasma acceleration, current sheet formation, applied field generation and mass injection and preionization, and are cast as specific prescriptions for the dynamic impedance, inductance change, circuit damping, plasma collisionality (or magnetization), magnetic field strength and topology, and intra-pulse sequencing.

I. Introduction

PULSED inductive plasma accelerators are electrodeless spacecraft propulsion devices which are capable of expelling propellants at high exhaust velocities ($\mathcal{O}$ (10 km/s)). This is accomplished when energy stored in a capacitor is discharged through an inductive coil, inducing a current in a plasma located near the face of the coil. The plasma current interacts with an induced magnetic field to accelerate the propellant and produce thrust.

Inductive plasma accelerators are attractive as propulsive devices for many reasons. The lifetime and contamination issues associated with electrode erosion in conventional plasma thrusters do not exist in devices where the discharge is inductively driven. In addition, a wider variety of propellants (e.g. CO_2, H_2O) becomes available for use when compatibility with metallic electrodes is no longer an issue. Moreover, all pulsed plasma accelerators can maintain the same performance level over a wide range of input power levels by adjusting the pulse rate.

Presently, there are two propulsion concepts in which interactions between induced magnetic fields and currents are used to accelerate propellant and produce thrust. One is the Pulsed Inductive Thruster (PIT),[1] in which both propellant ionization and acceleration are performed by the same pulse of current flowing through the inductive coil. In contrast, the Faraday Accelerator with Radio-frequency Assisted Discharge (FARAD)[2,3] uses a separate stage to preionize the propellant before it is accelerated by the current pulse in the coil. A schematic of this concept is presented in Fig. 1.

In a FARAD thruster, gas is injected into a preionization stage (injected from the left into the smaller tube in Fig. 1) and is ionized by a helicon discharge, which requires the applied axial magnetic field and an RF/helicon antenna; the latter is shown wrapped around the outside of the smaller tube. A helicon discharge[4–6] is a radio-frequency inductive discharge that is very efficient as a plasma source. The highly ionized plasma is guided by the applied magnetic field to flow radially outward as it exits the preionization stage.

A flat inductive coil is mounted on the outer side of the back-end (which protects the coil from the plasma). The coil extends from the outer radius of the central opening to the inner radius of the larger

*Graduate Research Assistant. Presently: Propulsion Research Scientist, NASA-MSFC, Huntsville, AL 35812. kurt.a.polzin@nasa.gov

†Chief Scientist at EPPDyL. Associate Professor, Applied Physics Group, Mechanical & Aerospace Engineering Dept. choueiri@princeton.edu

vessel and is referred to as the acceleration stage. A large azimuthal current, labeled J_{Coil} in Fig. 1, is quickly pulsed through the coil. The current sheet, shown as a thin disk in the figure, contains an induced azimuthal current, labeled J_{Plasma}, which flows in the opposite direction to the current in the coil. The induced current density interacts with the magnetic fields resulting in a Lorentz body force density.

Recent work[3] has shown that employing a separate preionization mechanism allows for the formation of an inductive current sheet at much lower discharge energies and voltages than those used in the PIT (∼50 J/pulse in the FARAD versus 4 kJ/pulse in the PIT). An additional conceptual difference between the two concepts is that in the FARAD the propellant is fed as a plasma from upstream of the acceleration stage whereas in the PIT a neutral gas is fed from downstream of the coil through a sizable nozzle.

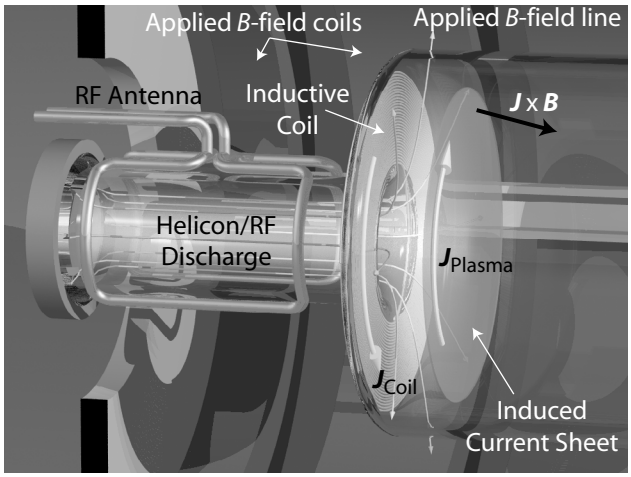

Figure 1. Schematic illustration of the FARAD concept.

Designs of pulsed inductive accelerators like the PIT are currently being performed using a set of empirical rules found to work over the years. The purpose of the present work is to state a set of rules and guidelines which can be directly applied to the design of a FARAD thruster. These rules are based upon existing empirical prescriptions as well as the insight resulting from recent experimental, theoretical and numerical investigations.[3,7] Some of the rules apply to pulsed inductive accelerators in general, while others are specifically tailored to the FARAD concept and geometry. The sections in the present work are organized along the lines of the physical processes present in a FARAD thruster. These are:

- Sect. II: Plasma acceleration,
- Sect. III: Current sheet formation,
- Sect. IV: Applied magnetic field generation,
- Sect. V: Mass injection and preionization.

In each section, a set of rules governing the optimization of the design will be outlined. Qualitatively, the rules fall roughly into one of three separate categories, depending upon the level of confidence and theoretical or experimental understanding of the physical processes.

- **Category A**: Rules which are directly supported by experimental results, solid theoretical modeling or knowledge of fundamental plasma physics processes.
- **Category B**: Rules which are supported by a combination of analytical and numerical modeling or are based upon general interpretations of plasma physics scaling relations.
- **Category C**: Rules which are speculative, or for which some inconclusive or ancillary evidence does exist.

The rules pertaining to each of the particular physical process are summarized and categorized according to these definitions at the end of each section.

II. Plasma Acceleration

A one-dimensional pulsed inductive plasma acceleration model consisting of a set of coupled circuit equations and a one-dimensional momentum equation has been developed by Lovberg and Dailey.[1,8] A lumped-element circuit model (see Fig. 2) is used to model the electrical characteristics of the accelerator. The external circuit (left side of the figure) possesses capacitance C, external inductance L_0, resistance R_e, and acceleration coil inductance L_C. The plasma also has an inductance equal to L_C and a resistance R_p. The two circuits are inductively coupled through the acceleration coil, which acts as a transformer with mutual inductance M. The value of M is a function of the current sheet position z.

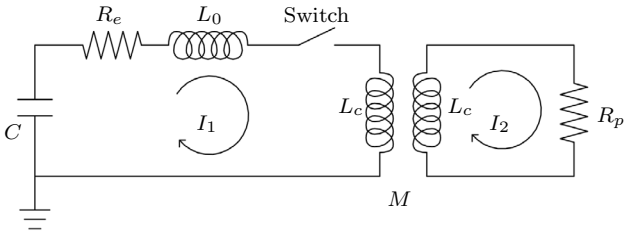

Figure 2. General lumped element circuit model of a pulsed inductive accelerator. (After Ref. [8])

In more recent work,[7] we nondimensionalized the acceleration model and identified several performance scaling parameters, which we briefly summarize here. The dynamic impedance parameter α represents the ratio of the resonant period of the unloaded circuit (i.e. period of the inductive thruster pulse when no plasma is present) to the time it takes for the circuit to double its initial inductance through motion of the plasma sheet. The inductance ratio L^* consists of the ratio of the initial inductance in the circuit to total the inductance change available to the circuit. Physically, L^* represents a measure of the fraction of energy that can be deposited into electromagnetic acceleration. The critical resistance ratios ψ_1 and ψ_2 (or $\Psi \equiv (\psi_1 + \psi_2)/2$) control the oscillatory nature of the current waveforms. The waveforms are underdamped for $\Psi < 1$ and approach the critically damped condition as $\Psi \to 1$.

The rules governing plasma acceleration are listed below and follow directly from the dimensionless acceleration model studies. The reader is referred to Ref. [7] for greater detail on the compositions and physical meanings of the dimensionless parameters.

- The discharge energy should be increased to raise the specific impulse, $I_{\rm sp}$, and the impulse bit. This is accomplished by increasing the value of the dynamic impedance parameter α. **(Category A)**
- The Lovberg criterion,[9] $\Delta L/L_0 = L^{*-1} > 1$ must be met for efficient electromagnetic acceleration. **(Category A)**
- The thickness of the propellant layer over the acceleration coil face should be much less than the characteristic electromagnetic coupling distance z_0 to increase the efficiency. Efficiency is maximized for a slug mass loading. **(Category A)**
- If the capacitor can handle higher levels of voltage ringing, the circuit parameters should be optimized such that the circuit is underdamped ($\Psi \equiv (\psi_1 + \psi_2)/2 < 1$) for greater thrust efficiency. **(Category B)**
- Exploration[7] of the nondimensional parameter space for typical conditions has indicated that the thrust efficiency tends to be highest in the vicinity of $\alpha \approx 2$. **(Category C)**

III. Current Sheet Formation

The most important assumption in the acceleration model we discussed in Ref. [7] is that current sheet formation is both immediate (at $t = 0$) and complete (does not allow the induced magnetic field to diffuse through it). This condition has proved most difficult to achieve experimentally. Unfortunately, when current sheet formation is delayed, data show[3,10] that a significant amount of the magnetic field energy radiates away from the acceleration coil and escapes without performing any useful acceleration.

Current sheet formation occurs more quickly as the accelerator coil current rise rate, dI/dt, is increased.[10] The increasing rise rate leads to the formation of a current sheet that more effectively contains the magnetic pressure radiating from the acceleration coil, leading to a more efficient acceleration process

For a given coil geometry, the simplest way to increase the current rise rate is to increase the ratio of the initial voltage to the initial (parasitic) inductance because the initial current rise rate scales like

$$\frac{dI}{dt} \propto \frac{V_0}{L_0}.$$

However, we are interested in a general rule that can be applied to a coil of arbitrary size. For this, we need to look not at the total current rise rate in the coil, but the linear current density rise rate. If we assume that

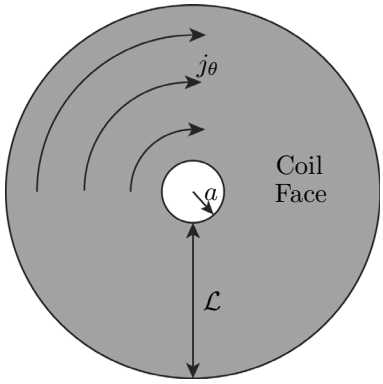

Figure 3. Schematic of a pulsed inductive accelerator coil face.

the linear current density in the coil, j_θ, is radially uniform over the coil face, then for a given coil dimension, $\mathcal{L}$ (see Fig. 3), the current density rise rate scales as

$$\frac{dj_\theta}{dt} \propto \frac{V_0}{L_0\,\mathcal{L}}.$$

In the PIT, the value of $V_0/(L_0\,\mathcal{L})$ is approximately equal to 1.5×10^{12} A/(m s). At this value, the current sheet in the PIT forms with little or no delay and is relatively impermeable to the induced magnetic field. The corresponding maximum value of $V_0/(L_0\,\mathcal{L})$ found in the FARAD proof-of-concept experiment[3] was 2.6×10^{11} A/(m s). At this current density rise rate, a current sheet formed in the FARAD, but it did not form very quickly and the experimental data indicate that it was still somewhat porous to both the propellant it encountered and the magnetic field induced by the acceleration coil.[3] This indicates that the rise rate should be further increased in future FARAD designs to levels closer to those found in the PIT to promote faster current sheet formation.

The rules governing current sheet formation in the FARAD are summarized as follows.

- Increasing the current rise rate in the coil leads to faster current sheet formation. For a given geometry, this is accomplished by increasing the ratio V_0/L_0. **(Category A)**
- The linear current density rise rate in the coil, which scales like $V_0/(L_0\,\mathcal{L})$, should have a value approaching 1.5×10^{12} A/(m s). **(Category C)**

IV. Applied Magnetic Field Generation

Optimization of the applied magnetic field is difficult because it is intimately connected to many of the physical processes in the FARAD, each having its own requirements. The applied field is necessary to generate a helicon plasma. It is also used to guide charged particles from the helicon source to the acceleration stage. Finally, it must not impede current sheet formation and allow for plasma detachment at the end of the acceleration coil pulse. In the present section, we discuss how each of these processes impacts the field optimization problem.

A. Helicon Source

To support the helicon discharge mode the field must be in the axial direction. We need not delve too deeply into the magnetic field scaling issues associated with the helicon discharge as they are beyond the scope of this paper and are, in fact, the subject of much research (see Refs. [4,5] and the references within). We should note, however, that helicon discharges at low pressures ($p < 5$ mTorr) have been sustained in a 50 G applied field while discharges at higher pressures ($p > 10$ mTorr) typically require field strengths on the order of several hundred gauss.[11]

B. Turning the Plasma

One of the difficulties inherent in the FARAD concept is transporting the propellant from the helicon source to the acceleration coil face. In the original concept,[2,3] it was envisioned that this difficulty could be overcome by exploiting the plasma's natural tendency to follow field lines, and employing an appropriately tailored magnetic field topology. This would be accomplished by creating an axial field in the helicon source that transitioned to a radial field and then passed over the face of the acceleration coil.

The strategy of using the magnetic field to turn the plasma is confounded if either: A) the plasma is not fully ionized or B) the ions are not magnetized and do not preferentially follow the field lines. We shall limit our ensuing discussion to two representative cases in an attempt to extract some meaningful design rules and constraints. In the first case we concern ourselves with a partially ionized plasma where the heavy species (ions and neutrals) acts as an unmagnetized fluid, while the electrons behave as magnetized particles. In the second case the plasma is fully ionized and both the ions and electrons act as magnetized particles.

1. Fluid Heavy Species/Magnetized Electrons

The fluid assumption for the heavy species (both ions and neutrals) implies that both are highly collisional and that the ions feel no impetus to preferentially follow the magnetic field lines. The ion Hall parameter

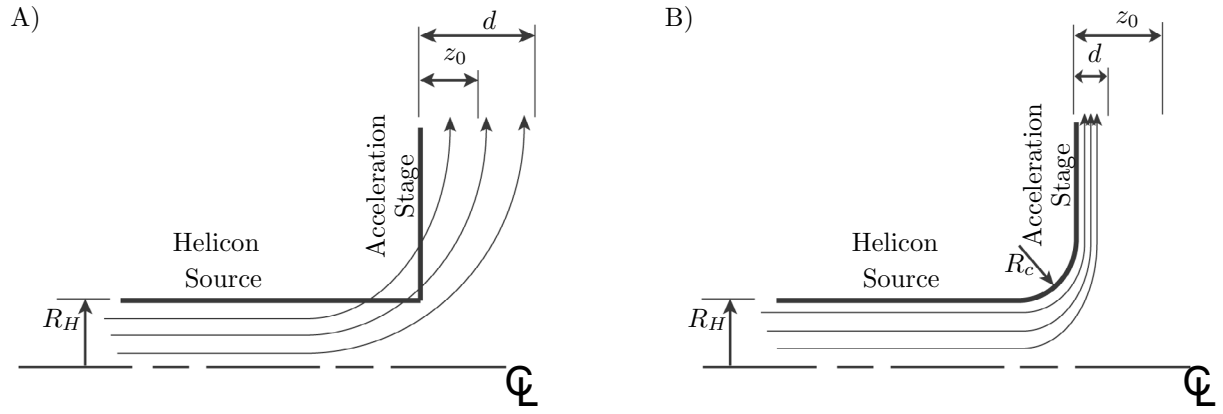

Figure 4. A) Schematic of the magnetic field topology in the FARAD proof-of-concept experiment from Ref. [2,3]. B) Optimized magnetic field topology

can be used to succinctly state this condition as

$$\Omega_{\mathrm{i}} = \frac{\omega_{\mathrm{ci}}}{\nu_{\mathrm{i}}} \ll 1,$$

where ω_{ci} is the ion cyclotron frequency and ν_{i} is the total ion collision frequency. The assumption of magnetized electrons implies

$$\Omega_{\mathrm{e}} = \frac{\omega_{\mathrm{ce}}}{\nu_{\mathrm{e}}} > 1.$$

However, even if the electron Hall parameter is large, electrons will only follow field lines if their cyclotron radii, r_{ce}, are smaller than the characteristic device length scales at every location in the system. In FARAD, the relevant length scales are: A) the helicon source radius, R_H, B) the acceleration stage propellant depth, d, and C) the radius of curvature of the transition between the two stages, R_c (see Fig. 4).

The highly mobile electrons are the primary current carriers in the plasma sheet.[12] This implies that the formation of a current sheet at lower discharge energies and voltages is facilitated by the coupling of the free electrons in the preionized plasma to the current pulse in the acceleration coil. Consequently, the applied magnetic field must be designed to deliver electrons from the helicon source to a narrow layer spatially located close to the acceleration coil face.

Two issues arose in the proof-of-concept experiment[3] which impeded the efficient transfer of electrons from the helicon source to the acceleration coil face, both of which are illustrated schematically in Fig. 4A. The first was that many of the magnetic field lines intersected with the sidewalls of the containment vessel. This resulted in a reduction of the number of electrons turned towards the coil face and led to a decrease of the preionized plasma density in the acceleration stage. The second problem was that the preionized plasma translated in the axial direction as it was moving radially over the acceleration coil, distributing itself over a wide volume of thickness d in the acceleration stage. Preionized plasma distributed outside the acceleration region (having length z_0) does not couple with the acceleration coil and is essentially wasted.

A more optimized design which seeks to address the problems listed above is presented in Fig. 4B. In this design, the transition between the helicon source and the acceleration stage is contoured so that the sidewalls do not intersect with the magnetic field lines. In addition, our recent acceleration modeling work[7] has shown that loading the propellant as a slug mass (i.e. as close as possible to the acceleration coil) results in the greatest thrust efficiency. We cannot turn the heavy species with the magnetic field in this case, but we can use the field topology illustrated in the figure to ensure that a dense layer of electrons of thickness $d < z_0$ resides at the coil face. Ideally, the heavy species could be turned by some other means so as to also reside in this layer, resulting in a mass loading approaching a slug mass.

2. Full Ionization/Magnetized Ions and Electrons

In this case, the electrons can be treated in the same fashion as before. On the other hand, since the ions are also magnetized in this case, they are subjected to the same conditions and constraints as the electrons.

Consequently, the ion Hall parameter must fulfill the inequality

$$\Omega_{\rm i} \gg 1$$

and the ion cyclotron radius must satisfy the conditions

$$r_{\rm ci} < R_H,\ R_c,\ d,$$

in each corresponding part of the thruster. If $d < z_0$, the plasma (both electrons and ions) will form a thin layer spatially located very close to the acceleration coil face. Under these conditions, the mass distribution should approach the desired slug mass loading.

As an aside, even if the conditions listed above are fulfilled, the axial field lines located near the centerline of the helicon stage may prove quite difficult to turn. Their tendency is to travel well beyond the acceleration stage before gradually sweeping around and reconnecting back on themselves. Also, the field is weaker at the centerline, making it more difficult to turn any ionized particles located there.

C. Sheet Formation and Detachment

As a general rule, the applied field in the acceleration region must not impede the formation of the current sheet and should not affect the acceleration process. In Ref. [13], inductive acceleration modeling resulted in the identification of a dimensionless parameter, γ, which could be recast to contain the apparent 'inductance' presented to the circuit by the applied magnetic field. Physically, γ is similar to α in that it represents the ratio of the resonant period of the unloaded circuit (i.e. period of the inductive thruster pulse when no plasma is present) to the time it takes for the circuit to double its initial inductance through motion of the plasma sheet. The difference is that the inductance change in α is attributable to the induced magnetic field, while γ takes into account the inductance changes associated with both the induced and applied magnetic fields.

Calculations revealed that the applied field did not have an effect on the acceleration process except in the region of parameter space where $\alpha < \mathcal{O}(1)$ and $\gamma > \mathcal{O}(0.01)$. Essentially, this corresponds to operation in a regime where the applied magnetic field strength approaches that of the induced field. It can also be thought of as a region where the inductance presented to the circuit by the applied field approaches the acceleration coil's inductance. This implies that the accelerator should operate in the regime where $\gamma < 0.01$ so the applied field will not affect the motion of the current sheet. This is equivalent to stating that the applied and induced magnetic field strengths should fulfill the inequality

$$B_{\rm r\ Applied} \ll B_{\rm r\ Induced}.$$

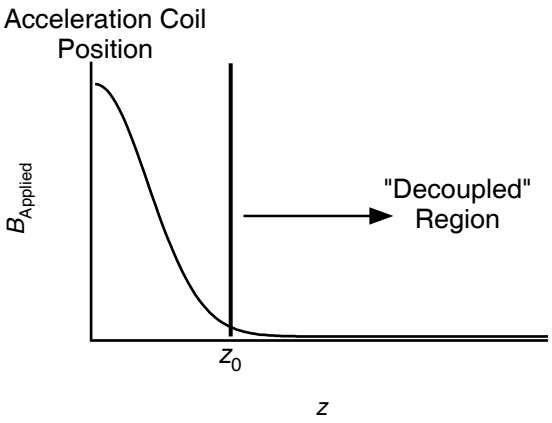

Figure 5. Conceptual graph showing the desired applied field strength as a function of position which will allow for plasma detachment.

We know from Sect. III that added inductance in the circuit slows the current sheet formation process and that this can lead to acceleration inefficiencies. We can assume that the applied field inductance affects the acceleration and current sheet formation processes equally (which is likely a good assumption since both processes are linear functions of inductance). Consequently, to maintain the current rise rate in the circuit, the applied field parameter should not exceed the threshold of $\gamma = 0.01$.

In an efficient acceleration, the current sheet should detach from the applied magnetic field and continue propagating away from the acceleration coil after the current pulse terminates. This will occur if by the end of the pulse the plasma reaches a region of space where the value of the applied magnetic field is small (≈ 0). This implies that the applied field in the acceleration region must possess a maximum value at the coil face and quickly decrease in magnitude as one moves away in the axial direction. The length scale over which this decrease should occur is the characteristic electromagnetic coupling distance, z_0. This condition can be stated succinctly through the inequality

$$\frac{B_{\rm r\ Applied}}{|\nabla B_{\rm r\ Applied}|} \ll z_0,$$

where the gradient is evaluated in the z-direction. A conceptual graph showing the field strength plotted as a function of position is presented in Fig. 5.

Summary of Design Rules for the Applied Field

We can compile the following design rules for the magnetic field to support a helicon discharge, turn the electrons effectively, and allow the current sheet to escape from the applied magnetic field once the acceleration coil is pulsed.

- The electrons must be magnetized to follow the field lines. Consequently, the conditions $\Omega_{\rm e} > 1$ and $r_{\rm ce} < R_H,\ R_c,\ d$ must be satisfied everywhere in the device. **(Category A)**
- Thrust efficiency is increased when the current sheet forms very close to the acceleration coil face. Therefore, the depth of the magnetic flux tubes passing over the acceleration coil face (which governs the electron layer depth and sheet initiation location) should be less than the characteristic electromagnetic coupling distance, $d < z_0$, and spatially located close to the coil's face. **(Category A)**
- To reduce plasma losses at the wall of the helicon source, the field topology and the walls of the device should be contoured in such a way that they do not intersect. **(Category A)**
- The applied axial field in the helicon section must be of sufficient strength, $\mathcal{O}(100)$ G, to support the helicon discharge mode. **(Category B)**
- To allow the plasma to effectively cross the applied magnetic field lines, the applied magnetic field strength and the peak induced magnetic field strength should satisfy the criteria $B_{\rm r\,Applied} \ll B_{\rm r\,Induced}$. **(Category B)**
- To allow for plasma 'detachment' once the acceleration pulse is complete, the applied field in the acceleration region should conform to the condition $B_{\rm r\ Applied}/|\nabla B_{\rm r\ Applied}| \ll z_0$. **(Category B)**
- To reduce the chance that the field will adversely affect the current sheet formation and acceleration processes, the maximum applied field strength in the acceleration stage should be such that the condition $\gamma < 0.01$ is fulfilled. **(Category C)**

If the plasma is fully ionized and the ions are also turned by the applied field, the following additional conditions must be fulfilled.

- The ions must be magnetized to follow the field lines. Consequently, the conditions $\Omega_{\rm i} \gg 1$ and $r_{\rm ci} < R_H,\ R_c,\ d$ must be satisfied everywhere in the device. **(Category A)**
- The depth of the magnetic flux tubes passing over the acceleration coil face (which governs the ion layer depth and mass distribution) should be less than the characteristic electromagnetic coupling distance ($d < z_0$), and it should also be spatially located near the coil face since thrust efficiency is maximized for a slug mass loading. **(Category A)**

V. Mass Injection and Preionization

There are three major pulsed systems in the FARAD (aside from the applied B-field coils, which may be pulsed in a real thruster). These are the gas valve, which introduces the initial propellant pulse into the thruster, the helicon source, which preionizes the gas, and the acceleration coil. The pulse length for each system and the intra-pulse sequencing are important from the point of view of mass utilization efficiency and, potentially, total power consumption.

The timing of the different pulsed systems is, in general, difficult to handle analytically. The thruster's dimensions and the prevailing state of the propellant, be it a partially ionized gas in which only the electrons are magnetized, or a fully ionized gas with magnetized ions and electrons, greatly affect the timing. The propellant valve and helicon source have finite response times which must be accounted for when determining the actual switch-on and switch-off times. Also, the convection speed of the propellant through the thruster may change, especially if it is appreciably heated in the helicon source. An additional complication arises if we were to consider that while the propellant pulse is convecting towards the acceleration stage, it is

also expanding through thermal diffusion. Finally, if the ions are magnetized, the changing magnetic field strength, which decreases as the field expands radially in the acceleration stage, may greatly affect the speed at which the ions expand over the acceleration stage face. The ions would experience an increase in velocity parallel to the magnetic field due to conservation of the first adiabatic invariant, μ, defined as

$$\mu = \frac{mv_{\perp}^2}{2B},$$

where $v_{\perp}$ is the velocity of an ion in the direction perpendicular to the applied magnetic field.

We should mention that in the case where the heavy species are acting as a fluid, the propellant (ions and neutrals) must somehow be turned so that they propagate radially along the face of the acceleration coil. This could be accomplished using some sort of physical nozzle or duct. However, we must keep in mind that the object's location in the plasma stream subjects it to constant bombardment and potential erosion. While this technique would turn the flow, the object may become a source of impurities or, even worse, be the life-limiting component in the system.

Considering the difficulty of arriving at an analytical prescription for optimizing the timing scheme for FARAD, the timing is perhaps best optimized experimentally using fast diagnostics (fast-response pressure gauges and/or Langmuir probes) located throughout the apparatus to monitor the spatial and temporal extent of the gas pulse.

We proceed with a general set of design rules which seek to guide the optimization of the intra-pulse sequencing.

- The neutral gas pulse, of temporal extent Δt_g, precedes the other pulses. The pulse length should be such that the propellant layer which reaches the acceleration stage completely fills the region between the inner and outer coil radii. The amount of additional propellant remaining outside that region constitutes a mass utilization inefficiency since it will not be accelerated when the acceleration circuit is pulsed. **(Category B)**

- The RF pulse length, Δt_{RF}, is the duration that power is supplied to the helicon stage. The RF pulse should not begin until the injected gas has filled the helicon stage. The pulse must remain active long enough to fill the entire acceleration stage with the preionized plasma but be deactivated before producing any extraneous plasma that may not reach the acceleration coil before it is pulsed. **(Category B)**

- The acceleration coil pulse, Δt_a, must not start until most of the preionized plasma has been guided to the back-end of the acceleration stage and completely fills the region between the inner and outer coil radii but it must begin before any significant portion of the leading edge of the preionized plasma begins escaping at the outer edge of the coil. **(Category B)**

- The thruster mass injection system should be spatially compact. This will not only save on thruster mass, but it will allow for a more repeatable mass injection and pulsing scheme by reducing the effects of longer timescale processes, such as thermal diffusion or recombination. The compact construction should lead to an overlap of the neutral gas and RF pulses. **(Category C)**

Before leaving this process, we should mention a few additional caveats which may be employed in a real thruster design. The demand for a fast gas valve can be alleviated by employing a burst-pulse scheme similar to that developed for gas-fed pulsed plasma thrusters.[14,15] In this mode, a "slow" and sturdy valve is operated at a low duty cycle and the thruster is operated in a burst of discharge pulses. If the response time of the RF-matching network is too slow to switch the preionization pulse on and off for each individual acceleration pulse, it too can operate at the lower duty cycle associated with the "slow" valve. The time between each consecutive *pulse* is equal to the time it takes the current sheet to sweep the gas through the thruster and then refill the acceleration region while the time between the *bursts* is dictated by the available steady-state power and the required (average) thrust. This technique would increase not only the mass utilization efficiency, but would also extend the lifetime of the system through the use of a lower repetition rate valve.

VI. Summary

We have presented a set of design rules and guidelines aimed at producing an efficient, high-performance thruster based upon the FARAD concept. The discussion was organized along the lines of the various physical processes present in the accelerator, with rules pertaining to a particular process collected in a series of statements at the end of the respective section. The rules are based on a combination of experimental results, analytical and numerical modeling, and physical intuition and we have assigned a qualitative measure of the level of confidence in each specific rule based upon the method of justification employed. A cursory examination of the various rules presented in each section show that some of the rules complement each other. Further experimental and theoretical studies would undoubtedly lead to a refinement of these rules.

Acknowledgments

The authors thank Dr. T.E. Markusic and Prof. K. Sankaran for several helpful discussions during the preparation of this manuscript. Support for Mr. Polzin's research partially provided by the National Defense Science and Engineering Graduate Fellowship Program.

References

[1]Dailey, C.L. and Lovberg, R.H., *The PIT MkV pulsed inductive thruster*, Tech. Rep. NASA CR-191155, TRW Systems Group, July 1993.

[2]Choueiri, E.Y. and Polzin, K.A., "Faraday acceleration with radio-frequency assisted discharge (FARAD)," 40^{th} *Joint Propulsion Conference*, Ft. Lauderdale, FL, July 11-14, 2004, AIAA 2004-3940.

[3]Choueiri, E.Y. and Polzin, K.A., "Faraday acceleration with radio-frequency assisted discharge," accepted for publication: *J. Propuls. Power*, Sept. 2005.

[4]Chen, F.F. and Boswell, R.W., "Helicons - The past decade," *IEEE Trans. Plasma Sci.*, Vol. **25**, No. 6, Dec. 1997, pp. 1245.

[5]Boswell, R.W. and Chen, F.F., "Helicons - The early years," *IEEE Trans. Plasma Sci.*, Vol. **25**, No. 6, Dec. 1997, pp. 1229.

[6]Lehane, J.A. and Thonemann, P.C., "An experimental study of helicon wave propagation in gaseous plasma," *Proc. Phys. Soc.*, Vol. **85**, 1965, pp. 301.

[7]Polzin, K.A. and Choueiri, E.Y., "Performance optimization criteria for pulsed inductive plasma acceleration," 41^{st} *Joint Propulsion Conference*, Tucson, AZ, July 10-13, 2005, AIAA 2005-3694. Also submitted for publication: *IEEE Trans. Plasma Sci.*, July 2005.

[8]Lovberg, R.H. and Dailey, C.L., "Large inductive thruster performance measurement," *AIAA Journal*, Vol. **20**, No. 7, July 1982, pp. 971–977.

[9]Lovberg, R.H., Hayworth, B.R., and Gooding, T., *The use of a coaxial plasma gun for plasma propulsion*, Tech. Rep. AE62-0678, G.D. Convair, May 1962.

[10]Dailey, C.L. and Lovberg, R.H., *PIT clamped discharge evolution*, Tech. Rep. AFOSR-TR-89-0130, TRW Space and Technology Group, Dec. 1988.

[11]Degeling, A.W., Jung, C.O., Boswell, R.W., and Ellingboe, A.R., "Plasma production from helicon waves," *Phys. Plasmas*, Vol. **3**, No. 7, July 1996, pp. 2788.

[12]Dailey, C.L. and Lovberg, R.H., "Current sheet structure in an inductive-impulsive plasma accelerator," *AIAA Journal*, Vol. **10**, No. 2, Feb. 1972, pp. 125–129.

[13]Polzin, K.A., *Investigations on the Faraday Accelerator with Radio-frequency Assisted Discharge*, Ph.D. thesis, Dept. of Mechanical and Aerospace Engineering, Princeton University, Princeton, NJ, 2005.

[14]Ziemer, J.K., Cubbin, E.A., Choueiri, E.Y., and Birx, D., "Performance Characterization of a High Efficiency Gas-Fed Pulsed Plasma Thruster," 33^{rd} *Joint Propulsion Conference*, Seattle, Washington, July 6-9, 1997, AIAA 97-2925.

[15]Ziemer, J.K., Choueiri, E.Y., and Birx, D., "Trends in performance improvements of a gas-fed pulsed plasma thruster," 25^{th} *International Electric Propulsion Conference*, Cleveland, OH, 1997, IEPC 97-040.